AD-A041 944 DIKEWOOD INDUSTRIES INC ALBUQUERQUE N MEX F/G 20/3
INTERACTION OF A RECTANGULAR FERRITE SLAB WITH MAGNETIC FIELDS.(U)
MAY 77 J LAM F29601-75-C-0120
UNCLASSIFIED DC-TN-1225-1 AFWL-TR-76-199 NL

1 OF 1
ADA041944

END

DATE FILMED
8 - 77

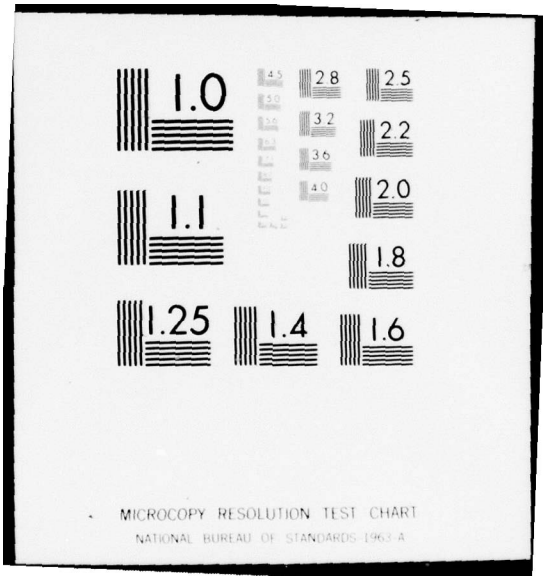
1.0
1.1
1.25
1.4
1.6
1.8
2.0
2.2
2.5
2.8
3.2
3.6
4.0
4.5
5.0
MICROCOPY RESOLUTION TEST CHART
NATIONAL BUREAU OF STANDARDS-1963-A

AFWL-TR-
76-199

(2)

INTERACTION OF A RECTANGULAR FERRITE SLAB WITH MAGNETIC FIELDS

Dikewood Industries, Inc.
1009 Bradbury Drive, S.E.
Albuquerque, NM 87106

May 1977

Final Report

Approved for public release; distribution unlimited.

AIR FORCE WEAPONS LABORATORY
Air Force Systems Command
Kirtland Air Force Base, NM 87117

AFWL-TR-76-199

This final report was prepared by Dikewood Industries, Inc, Albuquerque, New Mexico, under Contract F29601-75-C-0120, Job Order 12090503 with the Air Force Weapons Laboratory, Kirtland Air Force Base, New Mexico. Mr. William D. Prather (ELP) was the Laboratory Project Officer-in-Charge.

When US Government drawings, specifications, or other data are used for any purpose other than a definitely related Government procurement operation, the Government thereby incurs no responsibility nor any obligation whatsoever, and the fact that the Government may have formulated, furnished, or in any way supplied the said drawings, specifications, or other data, is not to be regarded by implication or otherwise, as in any manner licensing the holder or any other person or corporation, or conveying any rights or permission to manufacture, use, or sell any patented invention that may in any way be related thereto.

This report has been reviewed by the Information Office (OI) and is releasable to the National Technical Information Service (NTIS). At NTIS, it will be available to the general public, including foreign nations.

This technical report has been reviewed and is approved for publication.

William D Prather

WILLIAM D. PRATHER
Project Officer

FOR THE COMMANDER

Aaron B Loggins

AARON B. LOGGINS
Lt Colonel, USAF
Chief, Phenomenology and
Technology Branch

James L Griggs Jr.

JAMES L. GRIGGS, JR.
Colonel, USAF
Chief, Electronics Division

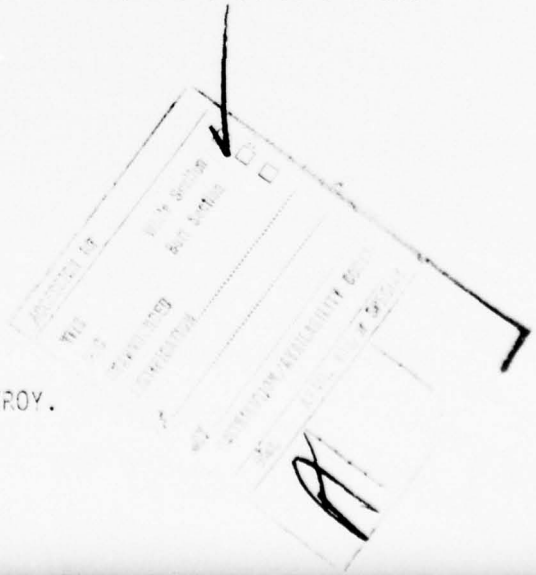

DO NOT RETURN THIS COPY. RETAIN OR DESTROY.

UNCLASSIFIED

SECURITY CLASSIFICATION OF THIS PAGE (When Data Entered)

REPORT DOCUMENTATION PAGE	READ INSTRUCTIONS BEFORE COMPLETING FORM
1. REPORT NUMBER: AFWL-TR-76-199	2. GOVT ACCESSION NO. / 3. RECIPIENT'S CATALOG NUMBER
4. TITLE (and Subtitle): INTERACTION OF A RECTANGULAR FERRITE SLAB WITH MAGNETIC FIELDS	5. TYPE OF REPORT & PERIOD COVERED: Final Report
	6. PERFORMING ORG. REPORT NUMBER: DC-TN-1225-1
7. AUTHOR(s): John Lam	8. CONTRACT OR GRANT NUMBER(s): F29601-75-C-0120
9. PERFORMING ORGANIZATION NAME AND ADDRESS: Dikewood Industries, Inc. 1009 Bradbury Drive, S.E. Albuquerque, NM 87106	10. PROGRAM ELEMENT, PROJECT, TASK AREA & WORK UNIT NUMBERS: 64747F 12090503
11. CONTROLLING OFFICE NAME AND ADDRESS: Air Force Weapons Laboratory (ELP) Kirtland Air Force Base, NM 87117	12. REPORT DATE: May 1977
	13. NUMBER OF PAGES: 40
14. MONITORING AGENCY NAME & ADDRESS (if different from Controlling Office)	15. SECURITY CLASS. (of this report): UNCLASSIFIED
	15a. DECLASSIFICATION/DOWNGRADING SCHEDULE

16. DISTRIBUTION STATEMENT (of this Report)

Approved for public release; distribution unlimited.

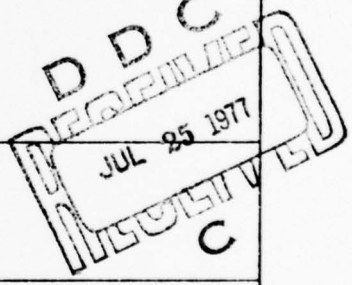

17. DISTRIBUTION STATEMENT (of the abstract entered in Block 20, if different from Report)

18. SUPPLEMENTARY NOTES

19. KEY WORDS (Continue on reverse side if necessary and identify by block number)

Electromagnetic fields and waves — EC-135
Antennas — E-4
Ferrite

20. ABSTRACT (Continue on reverse side if necessary and identify by block number)

The general problem of a permeable body in external magnetic fields is formulated as a two-dimensional Fredholm integral equation of the second kind. Using the method of averaging functional corrections, the equation is solved approximately for a highly-permeable rectangular solid (a) in a uniform field and (b) in the field of a rectangular current loop wound around the midsection of the solid. A large magnetic flux concentration is found in both cases for a thin solid. The results are applicable to the analysis of an aircraft VLF magnetic loop receiving antenna.

DD FORM 1 JAN 73 1473 EDITION OF 1 NOV 65 IS OBSOLETE

UNCLASSIFIED

SECURITY CLASSIFICATION OF THIS PAGE (When Data Entered)

112850

TABLE OF CONTENTS

ILLUSTRATIONS

SECTION I

INTRODUCTION

One VLF magnetic loop receiving antenna on the EC-135 aircraft consists of two orthogonal conductor coils wound around a rectangular slab made up of two arrays of thin ferrite rods. The rod assembly is mounted flat on the metallic skin of the fuselage. Essentially the function of the ferrite is to concentrate the magnetic flux of the incoming VLF signal. The receiving antenna is completely characterized by (a) the input impedance Z_{in} which is mainly the coil self-inductance, and (b) the open-circuit voltage V_{oc} which is proportional to the magnetic flux. These two quantities can be calculated by solving two quasistatic boundary value problems of a rectangular ferrite slab in applied magnetic fields.

In this report the general problem of a permeable body in an external quasistatic magnetic field is first formulated as a Fredholm integral equation of the second kind. For a uniform external field this integral equation is solved approximately by the method of averaging functional corrections [1]. The flux enhancement factor of a highly-permeable rectangular slab is determined for a wide range of the thickness-to-length ratio. The same approximation method is also used to calculate the self-inductance of a thin-wire current loop wound around the mid-section of the rectangular slab.

SECTION II

GENERAL INTEGRAL-EQUATION FORMULATION

Let there be a static magnetic field $\underline{H}^{inc}(\underline{r})$ in free space. Suppose a finite solid of uniform permeability μ is introduced into this field. We wish to calculate the induced field $\underline{H}^{ind}(\underline{r})$.

Let the space outside the permeable solid be designated as region 1 and that inside as region 2. Then on the surface S of the solid, the total magnetic field

$$\underline{H}^{tot}(\underline{r}) = \underline{H}^{inc}(\underline{r}) + \underline{H}^{ind}(\underline{r}) \tag{1}$$

satisfies the two boundary conditions for the tangential and normal components:

$$H_{1t}^{ind}(\underline{r}) = H_{2t}^{ind}(\underline{r}) \tag{2}$$

$$\mu_o\left[H_n^{inc}(\underline{r}) + H_{1n}^{ind}(\underline{r})\right] = \mu\left[H_n^{inc}(\underline{r}) + H_{2n}^{ind}(\underline{r})\right] \tag{3}$$

We introduce the induced magnetostatic potential $\phi^{ind}(\underline{r})$ such that

$$\underline{H}^{ind}(\underline{r}) = -\nabla\phi^{ind}(\underline{r}) \tag{4}$$

The conditions (2) and (3) then imply that $\phi^{ind}(\underline{r})$ is continuous across the boundary S but that its normal derivative has a discontinuity. It is well known that these behaviors are inherent in the integral representation

$$\phi^{ind}(\underline{r}) = \frac{1}{4\pi}\int_S \frac{\rho_m(\underline{r}')}{|\underline{r} - \underline{r}'|}\,dS \tag{5}$$

for $\underline{r}$ lying both inside and outside the solid. That is to say, the induced potential is considered to arise from induced magnetic charges of surface density $\rho_m(\underline{r})$ on the solid's surface. Expression (5) is clearly a solution of the Laplace equation.

The induced magnetic field is given by (4) and (5). As the field point $\underline{r}$ approaches the surface S we have the following two well-known limits in potential theory [2]:

$$H_{1n}^{ind}(\underline{r}) = \frac{1}{2}\rho_m(\underline{r}) - \frac{1}{4\pi} P \int_S \rho_m(\underline{r}') \frac{\partial}{\partial n}\left(\frac{1}{|\underline{r} - \underline{r}'|}\right) dS$$

$$H_{2n}^{ind}(\underline{r}) = -\frac{1}{2}\rho_m(\underline{r}) - \frac{1}{4\pi} P \int_S \rho_m(\underline{r}') \frac{\partial}{\partial n}\left(\frac{1}{|\underline{r} - \underline{r}'|}\right) dS \qquad (6)$$

where $\underline{n}$ denotes the outward normal at the field point $\underline{r}$ on S. The symbol P in front of the integral denotes the Cauchy principal value whereby we must exclude from the integral an infinitesimally small circular disk centered at $\underline{r}$. It is precisely the integration over this disk that gives rise to the term $\pm\frac{1}{2}\rho_m(\underline{r})$ in (6). Substituting (6) into (3) we obtain a Fredholm integral equation of the second kind for the induced charge density $\rho_m(\underline{r})$ [3]:

$$\rho_m(\underline{r}) + \frac{\mu - \mu_o}{\mu + \mu_o}\frac{1}{2\pi} P \int_S \rho_m(\underline{r}') \frac{\partial}{\partial n}\left(\frac{1}{|\underline{r} - \underline{r}'|}\right) dS = \frac{\mu - \mu_o}{\mu + \mu_o} 2H_n^{inc}(\underline{r}) \qquad (7)$$

The solution is closely related to the total normal magnetic induction on S. Eliminating the integral between (6) and (7) we obtain

$$B_{2n}^{tot}(\underline{r}) = \mu\left[H_n^{inc}(\underline{r}) + H_{2n}^{ind}(\underline{r})\right] = \frac{\mu\mu_o}{\mu - \mu_o}\rho_m(\underline{r}) \qquad (8)$$

SECTION III

RECTANGULAR SOLID IN A UNIFORM FIELD

Let us specialize the integral equation (7) to the case of a highly-permeable rectangular solid placed in a uniform magnetic field. The situation is depicted in Fig. 1. We set up a rectangular coordinate system such that the origin coincides with the center of the solid and that the coordinate axes are parallel to its edges. Let the edges parallel to the x, y and z directions be, respectively, 2a, 2b and 2c in length. Hence the six faces of the solid are defined by $x = \pm a$, $y = \pm b$ and $z = \pm c$. Since any uniform field can be resolved into three independent orthogonal components, we can, without loss of generality, take the incident magnetic field to point in the positive x direction.

From the symmetry of the problem we need only consider the values of $\rho_m(\underline{r})$ on three faces of the solid. It is convenient to introduce three functions f, g and h such that

$$\rho_m(\underline{r}) = \begin{cases} f(x, y) & z = \pm c \\ \pm g(y, z) & x = \pm a \\ h(z, x) & y = \pm b \end{cases} \tag{9}$$

These functions are odd in x and even in y and z. In practice, the permeability μ is usually made very high, so that the factor $(\mu - \mu_o)/(\mu + \mu_o)$ in (7) can in most cases be replaced by 1. For example, if $\mu > 100\mu_o$, this factor differs from 1 by less than 1%. Furthermore we define $\underline{H}^{inc}(\underline{r}) = H_o \underline{e}_x$, where $\underline{e}_x$ denotes the unit vector in the x-direction. Then (7) is equivalent to the set of three coupled integral equations:

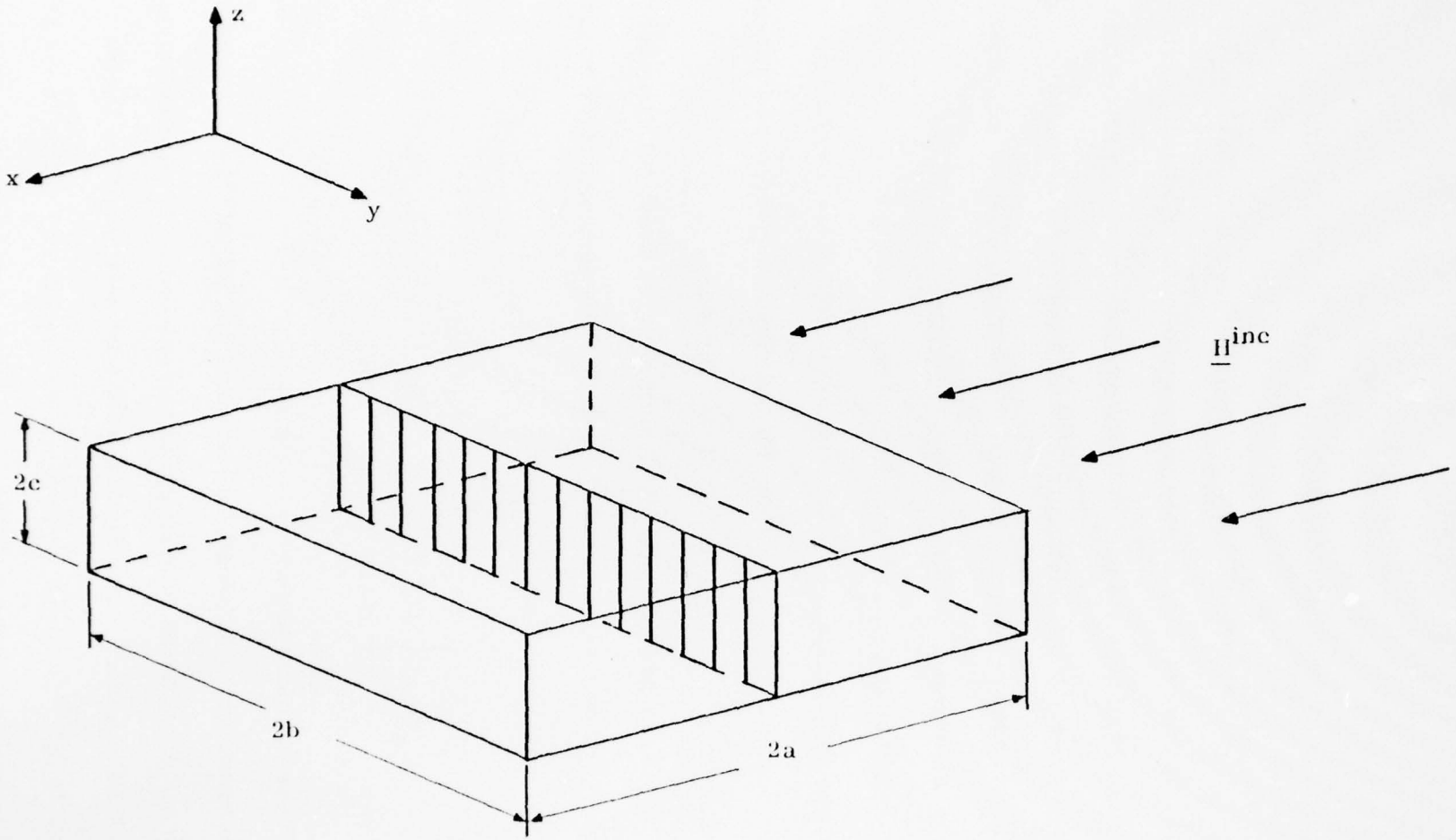

Figure 1. Geometry of the Problem

$$f(x, y) - \frac{1}{2\pi}\int_{-a}^{a} dx' \int_{-b}^{b} dy'\, f(x', y') \frac{2c}{\left[(x - x')^2 + (y - y')^2 + 4c^2\right]^{3/2}}$$

$$- \frac{1}{2\pi}\int_{-b}^{b} dy' \int_{-c}^{c} dz'\, g(y', z') \left(\frac{c - z'}{\left[(x - a)^2 + (y - y')^2 + (c - z')^2\right]^{3/2}} \right.$$

$$\left. - \frac{c - z'}{\left[(x + a)^2 + (y - y')^2 + (c - z')^2\right]^{3/2}} \right)$$

$$- \frac{1}{2\pi}\int_{-c}^{c} dz' \int_{-a}^{a} dx'\, h(z', x') \left(\frac{c - z'}{\left[(x - x')^2 + (y - b)^2 + (c - z')^2\right]^{3/2}} \right.$$

$$\left. + \frac{c - z'}{\left[(x - x')^2 + (y + b)^2 + (c - z')^2\right]^{3/2}} \right) = 0 \tag{10}$$

$$g(y, z) - \frac{1}{2\pi}\int_{-b}^{b} dy' \int_{-c}^{c} dz'\, g(y', z') \frac{-2a}{\left[4a^2 + (y - y')^2 + (z - z')^2\right]^{3/2}}$$

$$- \frac{1}{2\pi}\int_{-a}^{a} dx' \int_{-b}^{b} dy'\, f(x', y') \left(\frac{a - x'}{\left[(a - x')^2 + (y - y')^2 + (z - c)^2\right]^{3/2}} \right.$$

$$\left. + \frac{a - x'}{\left[(a - x')^2 + (y - y')^2 + (z + c)^2\right]^{3/2}} \right)$$

$$- \frac{1}{2\pi}\int_{-c}^{c} dz' \int_{-a}^{a} dx'\, h(z', x') \left(\frac{a - x'}{\left[(a - x')^2 + (y - b)^2 + (z - z')^2\right]^{3/2}} \right.$$

$$\left. + \frac{a - x'}{\left[(a - x')^2 + (y + b)^2 + (z - z')^2\right]^{3/2}} \right) = 2H_o \tag{11}$$

$$h(z, x) - \frac{1}{2\pi} \int_{-c}^{c} dz' \int_{-a}^{a} dx' \, h(z', x') \frac{2b}{\left[(x - x')^2 + 4b^2 + (z - z')^2\right]^{3/2}}$$

$$- \frac{1}{2\pi} \int_{-a}^{a} dx' \int_{-b}^{b} dy' \, f(x', y') \left(\frac{b - y'}{\left[(x - x')^2 + (b - y')^2 + (z - c)^2\right]^{3/2}} \right.$$

$$\left. + \frac{b - y'}{\left[(x - x')^2 + (b - y')^2 + (z + c)^2\right]^{3/2}} \right)$$

$$- \frac{1}{2\pi} \int_{-b}^{b} dy' \int_{-c}^{c} dz' \, g(y', z') \left(\frac{b - y'}{\left[(x - a)^2 + (b - y')^2 + (z - z')^2\right]^{3/2}} \right.$$

$$\left. - \frac{b - y'}{\left[(x + a)^2 + (b - y')^2 + (z - z')^2\right]^{3/2}} \right) = 0 \tag{12}$$

Note that the principal value integral in (7) vanishes when both $\underline{r}$ and $\underline{r}'$ lie on the same flat surface.

In practice we are often interested only in the total magnetic flux passing through the midsection of the solid shown as the shaded area in Fig. 1. This total flux is

$$\Phi = \int_{-b}^{b} dy \int_{-c}^{c} dz \, B_{2x}^{tot}(x = 0) \tag{13}$$

Since $\underline{B}$ is divergenceless, each flux line crossing the shaded area must eventually come out through the faces of the solid for $x > 0$. Therefore (13) can also be written as

$$\Phi = 2\int_0^a dx \int_{-b}^b dy\, B_{2z}^{tot}(z = c) + \int_{-b}^b dy \int_{-c}^c dz\, B_{2x}^{tot}(x = a)$$

$$+ 2\int_{-c}^c dz \int_0^a dx\, B_{2y}^{tot}(y = b) \tag{14}$$

If we introduce the average values

$$\overline{f} = \frac{1}{2ab}\int_0^a dx \int_{-b}^b dy\, f(x, y)$$

$$\overline{g} = \frac{1}{4bc}\int_{-b}^b dy \int_{-c}^c dz\, g(y, z) \tag{15}$$

$$\overline{h} = \frac{1}{2ca}\int_{-c}^c dz \int_0^a dx\, h(z, x)$$

then by (8) and (9), for $\mu >> \mu_o$, expression (14) simplifies to

$$\Phi = 4ab\mu_o\left(\overline{f} + \frac{c}{a}\overline{g} + \frac{c}{b}\overline{h}\right) \tag{16}$$

SECTION IV

METHOD OF AVERAGING FUNCTIONAL CORRECTIONS

We have on hand a rather formidable system of coupled two-dimensional integral equations in (10), (11) and (12). One method to derive an approximate solution is obviously to replace these equations with a set of algebraic equations by applying a suitable numerical integration formula. And yet, in practice, unless the problem exhibits a large amount of symmetry, as in the case of the electrostatic analog of a dielectric cube [4], we have to set up quite a large number of algebraic equations in order to obtain reasonable accuracy. Their solution is likely to tax severely the capacity of all but the largest computers. This undesirable state of affairs is especially true of the inductance calculations in later sections, where the incident magnetic field is not uniform but rather produced by a current-carrying thin wire wound around the rectangular solid. A purely numerical solution will be greatly disadvantaged since the field is singular at the wire, and a high-order numerical integration formula must be used to ensure good accuracy.

In this work we shall employ an analytical approximation procedure known as the method of averaging functional corrections [1]. Essentially this method consists of a self-consistent iterative calculation of the average values of the unknown functions over the intervals of integration. As such, it is ideally suited to calculating the total flux in (16), since in each order of the iteration the method yields directly the average values $\bar{f}$, $\bar{g}$ and $\bar{h}$.

The method of averaging functional corrections is actually quite simple in principle. In the first approximation we replace f, g and h under the integrals in (10), (11) and (12) by their average values defined in (15). Specifically we let

$$f(x', y') \rightarrow \begin{cases} \overline{f} & x' > 0 \\ -\overline{f} & x' < 0 \end{cases}$$

$$g(y', z') \rightarrow \overline{g}$$

$$h(z', x') \rightarrow \begin{cases} \overline{h} & x' > 0 \\ -\overline{h} & x' < 0 \end{cases} \tag{17}$$

since f and h are both odd in x'. Under these replacements, the three equations (10), (11) and (12) can be subsumed under the matrix equation

$$F - \frac{1}{2\pi} K \cdot \overline{F} = F_o \tag{18}$$

where

$$F = \begin{pmatrix} f(x, y) \\ g(y, z) \\ h(z, x) \end{pmatrix} , \qquad \overline{F} = \begin{pmatrix} \overline{f} \\ \overline{g} \\ \overline{h} \end{pmatrix} , \qquad F_o = \begin{pmatrix} 0 \\ 2H_o \\ 0 \end{pmatrix} \tag{19}$$

and K is a 3×3 matrix with elements

$$K_{11}(x, y) = \int_0^a dx' \int_{-b}^b dy' \left(\frac{2c}{\left[(x - x')^2 + (y - y')^2 + 4c^2 \right]^{3/2}} - \frac{2c}{\left[(x + x')^2 + (y - y')^2 + 4c^2 \right]^{3/2}} \right)$$

$$K_{12}(x, y) = \int_{-b}^{b} dy' \int_{-c}^{c} dz' \left(\frac{c - z'}{\left[(x - a)^2 + (y - y')^2 + (c - z')^2\right]^{3/2}} \right.$$

$$\left. - \frac{c - z'}{\left[(x + a)^2 + (y - y')^2 + (c - z')^2\right]^{3/2}} \right)$$

$$K_{13}(x, y) = \int_{-c}^{c} dz' \int_{0}^{a} dx' \left(\frac{c - z'}{\left[(x - x')^2 + (y - b)^2 + (c - z')^2\right]^{3/2}} \right.$$

$$- \frac{c - z'}{\left[(x + x')^2 + (y - b)^2 + (c - z')^2\right]^{3/2}}$$

$$+ \frac{c - z'}{\left[(x - x')^2 + (y + b)^2 + (c - z')^2\right]^{3/2}}$$

$$\left. - \frac{c - z'}{\left[(x + x')^2 + (y + b)^2 + (c - z')^2\right]^{3/2}} \right)$$

$$K_{21}(y, z) = \int_{0}^{a} dx' \int_{-b}^{b} dy' \left(\frac{a - x'}{\left[(a - x')^2 + (y - y')^2 + (z - c)^2\right]^{3/2}} \right.$$

$$- \frac{a + x'}{\left[(a + x')^2 + (y - y')^2 + (z - c)^2\right]^{3/2}}$$

$$+ \frac{a - x'}{\left[(a - x')^2 + (y - y')^2 + (z + c)^2\right]^{3/2}}$$

$$\left. - \frac{a + x'}{\left[(a + x')^2 + (y - y')^2 + (z + c)^2\right]^{3/2}} \right)$$

$$K_{22}(y,z) = -\int_{-b}^{b} dy' \int_{-c}^{c} dz' \frac{2a}{\left[4a^2 + (y-y')^2 + (z-z')^2\right]^{3/2}}$$

$$K_{23}(y,z) = \int_{-c}^{c} dz' \int_{0}^{a} dx' \left(\frac{a-x'}{\left[(a-x')^2 + (y-b)^2 + (z-z')^2\right]^{3/2}} \right.$$

$$- \frac{a+x'}{\left[(a+x')^2 + (y-b)^2 + (z-z')^2\right]^{3/2}}$$

$$+ \frac{a-x'}{\left[(a-x')^2 + (y+b)^2 + (z-z')^2\right]^{3/2}}$$

$$\left. - \frac{a+x'}{\left[(a+x')^2 + (y+b)^2 + (z-z')^2\right]^{3/2}} \right)$$

$$K_{31}(z,x) = \int_{0}^{a} dx' \int_{-b}^{b} dy' \left(\frac{b-y'}{\left[(x-x')^2 + (b-y')^2 + (z-c)^2\right]^{3/2}} \right.$$

$$- \frac{b-y'}{\left[(x+x')^2 + (b-y')^2 + (z-c)^2\right]^{3/2}}$$

$$+ \frac{b-y'}{\left[(x-x')^2 + (b-y')^2 + (z+c)^2\right]^{3/2}}$$

$$\left. - \frac{b-y'}{\left[(x+x')^2 + (b-y')^2 + (z+c)^2\right]^{3/2}} \right)$$

$$K_{32}(z,x) = \int_{-b}^{b} dy' \int_{-c}^{c} dz' \left(\frac{b - y'}{\left[(x - a)^2 + (b - y')^2 + (z - z')^2\right]^{3/2}} - \frac{b - y'}{\left[(x + a)^2 + (b - y')^2 + (z - z')^2\right]^{3/2}} \right)$$

$$K_{33}(z,x) = \int_{-c}^{c} dz' \int_{0}^{a} dx' \left(\frac{2b}{\left[(x - x')^2 + 4b^2 + (z - z')^2\right]^{3/2}} - \frac{2b}{\left[(x + x')^2 + 4b^2 + (z - z')^2\right]^{3/2}} \right) \qquad (20)$$

These matrix elements are explicitly odd in x and even in y and z. The averages $\bar{f}$, $\bar{g}$ and $\bar{h}$, up to now unknown, can be determined self-consistently by evaluating the average of (18). A set of three linear algebraic equations result:

$$\left(1 - \frac{1}{2\pi}\bar{K}\right) \cdot \bar{F} = \bar{F}_o \qquad (21)$$

We have introduced the obvious notations

$$\bar{K}_{1i} = \frac{1}{ab} \int_0^a dx \int_0^b dy \, K_{1i}(x,y)$$

$$\bar{K}_{2i} = \frac{1}{bc} \int_0^b dy \int_0^c dz \, K_{2i}(y,z) \qquad i = 1, 2, 3$$

$$\bar{K}_{3i} = \frac{1}{ca} \int_0^c dz \int_0^a dx \, K_{3i}(z,x) \qquad (22)$$

Substituting (21) into (18), we obtain the first iterated solution of (10), (11) and (12):

$$F = F_o + \frac{1}{2\pi} K \cdot \left(1 - \frac{1}{2\pi}\overline{K}\right)^{-1} \cdot \overline{F}_o \tag{23}$$

In the present case $\overline{F}_o = F_o$.

There are systematic procedures to improve the solution by iteration. But in the present work we shall not go beyond the first iterated solution (23). We can expect considerable local difference between the exact solution and (23) at various points on the surface of the rectangular solid. On the other hand we are interested mainly in the total flux (16) which is a global quantity and is obtained by integrating the induced magnetic charge over the solid's surface. We believe (21) gives us a good approximation to the flux. The present situation may be compared with that of calculating the capacitance of a conductor where a rough approximation to the surface charge density often leads to an accurate value for the capacitance. Our approximation scheme is akin to the Hartree-Fock approximation in atomic structure calculations and the Vlasov approximation in plasma dynamics. The idea is to replace an unknown local or microscopic quantity under an integral by its global or macroscopic average. This average is then calculated self-consistently from the integral or integro-differential equation thus approximated.

For a detailed discussion on deriving higher-order approximations as well as on all other aspects of the method of averaging functional

corrections, the reader is referred to the monograph of Luchka [1]. In this book the method is attributed to Yu. D. Sokolov.

SECTION V

NUMERICAL RESULTS OF FLUX CALCULATIONS

The flux Φ can be obtained from (16) and (21) by working out the averaged matrix $\overline{K}$. Its nine elements are really four-dimensional integrals. Let us first evaluate the set of nine two-dimensional integrals K in (20). It is clear that this is an enterprise that takes anybody no small amount of effort. We shall not write out the results as they are exceedingly lengthy, but shall only note that they can be expressed in terms of the following four types of integrals:

$$\int_0^a dx' \int_{-b}^b dy' \frac{C}{\left[(x - x')^2 + (y - y')^2 + C^2\right]^{3/2}}$$

$$= \tan^{-1} \frac{(x - a)(y - b)}{C\left[(x - a)^2 + (y - b)^2 + C^2\right]^{1/2}} - \tan^{-1} \frac{x(y - b)}{C\left[x^2 + (y - b)^2 + C^2\right]^{1/2}}$$

$$- \tan^{-1} \frac{(x - a)(y + b)}{C\left[(x - a)^2 + (y + b)^2 + C^2\right]^{1/2}} + \tan^{-1} \frac{x(y + b)}{C\left[x^2 + (y + b)^2 + C^2\right]^{1/2}}$$

$$\int_{-b}^b dy' \int_{-c}^c dz' \frac{z - z'}{\left[A^2 + (y - y')^2 + (z - z')^2\right]^{3/2}}$$

$$= \ell n \left(\frac{\left[A^2 + (y+b)^2 + (z - c)^2\right]^{1/2} + y + b}{\left[A^2 + (y+b)^2 + (z + c)^2\right]^{1/2} + y + b} \cdot \frac{\left[A^2 + (y - b)^2 + (z + c)^2\right]^{1/2} + y - b}{\left[A^2 + (y - b)^2 + (z - c)^2\right]^{1/2} + y - b} \right)$$

$$\int_{-c}^{c} dz' \int_{0}^{a} dx' \frac{z - z'}{\left[(x - x')^2 + B^2 + (z - z')^2\right]^{3/2}}$$

$$= \ell n \left(\frac{\left[x^2 + B^2 + (z - c)^2\right]^{1/2} + x}{\left[x^2 + B^2 + (z + c)^2\right]^{1/2} + x} \cdot \frac{\left[(x - a)^2 + B^2 + (z + c)^2\right]^{1/2} + x - a}{\left[(x - a)^2 + B^2 + (z - c)^2\right]^{1/2} + x - a} \right)$$

$$\int_{0}^{a} dx' \int_{-b}^{b} dy' \frac{x - x'}{\left[(x - x')^2 + (y - y')^2 + C^2\right]^{3/2}}$$

$$= \ell n \left(\frac{\left[x^2 + (y - b)^2 + C^2\right]^{1/2} + y - b}{\left[x^2 + (y + b)^2 + C^2\right]^{1/2} + y + b} \cdot \frac{\left[(x - a)^2 + (y + b)^2 + C^2\right]^{1/2} + y + b}{\left[(x - a)^2 + (y - b)^2 + C^2\right]^{1/2} + y - b} \right) \quad (24)$$

Next we must integrate these complicated expressions over the solid's surface to calculate $\overline{K}$, in accordance with (22). The integrals can probably be done analytically, but the amount of algebra involved must be truly enormous. Since the expressions (24) have only logarithmic singularities at the edges of the solid, we decide to perform the remaining two-dimensional integrations numerically.

For a case of immediate practical interest, we choose a = b and define a thickness-to-length ratio

$$\kappa = \frac{c}{a} \quad (25)$$

The values of $\overline{K}$ for various κ are shown in Table 1. Note that $\overline{K}_{22}$ is negative. Then $\overline{f}$, $\overline{g}$ and $\overline{h}$ can be obtained by solving the set of three linear algebraic equations (21). The solutions are shown in Table 2 together with the flux enhancement factor Φ/Φ_o, where

$$\Phi_o = 4bc\mu_o H_o \tag{26}$$

is the total incident flux through the shaded area in Fig. 1 in the absence of the rectangular solid. The ratio Φ/Φ_o is also plotted versus κ in Figs. 2 and 3. We see that there is a dramatic flux enhancement for a thin rectangular slab. But the divergence of Φ/Φ_o at small κ can only be logarithmic. This becomes evident when we plot out the quantity $\kappa\Phi/\Phi_o$ in Fig. 4 and find that it approaches 0 with κ. Since, by (25) and (26),

$$\kappa \frac{\Phi}{\Phi_o} = \frac{\Phi}{4a^2\mu_o H_o} \qquad a = b \tag{27}$$

it is really the total flux in units of $4a^2\mu_o H_o$.

For the case of a cube ($\kappa = 1$), we obtain a value of 3.57 for Φ/Φ_o. This may be compared with the exact value of 3 for an infinitely permeable sphere. The value for a cube is bigger probably because of the edges and corners. We have also applied the method of averaging functional corrections to the integral equation for a sphere. Comparing the first iterated solution with the exact result, we find that the total flux is smaller than the exact value by about 8.3%. We hazard a guess that our flux results in Table 2 are smaller than the exact values by about 10%.

Table 1. Elements of the averaged matrix $\overline{K}$ as a function of $\kappa = c/a$ for $a = b$

κ	.01	.02	.04	.06	.08	.1	.2	.4	.6	.8	1.
$\overline{K}_{11}$	5.604	5.144	4.439	3.892	3.443	3.065	1.809	.7279	.3310	.1656	.0896
$\overline{K}_{12}$	.0568	.1157	.2275	.3321	.4302	.5223	.9053	1.388	1.643	1.782	1.860
$\overline{K}_{13}$	.0552	.1102	.2102	.2990	.3786	.4504	.7224	1.015	1.151	1.221	1.260
$\overline{K}_{21}$	16.47	13.72	10.99	9.415	8.312	7.469	4.970	2.836	1.884	1.371	1.063
$-\overline{K}_{22}$	.0083	.0166	.0331	.0497	.0662	.0827	.1642	.3202	.4622	.5877	.6967
$\overline{K}_{23}$	.0912	.1593	.2679	.3557	.4300	.4945	.7230	.9437	1.029	1.058	1.063
$\overline{K}_{31}$	15.61	12.90	10.24	8.736	7.699	6.918	4.677	2.845	2.022	1.556	1.260
$\overline{K}_{32}$	.1020	.1809	.3110	.4202	.5159	.6017	.9343	1.345	1.590	1.749	1.860
$\overline{K}_{33}$	.0012	.0023	.0046	.0069	.0093	.0115	.0229	.0440	.0622	.0774	.0896

Table 2. Magnetic flux enhancement factor Φ/Φ_o as a function of $\kappa = c/a$ for $a = b$ and $\mu = \infty$

κ	.01	.02	.04	.06	.08	.1	.2	.4	.6	.8	1.
$\bar{f}/H_o$	.296	.367	.443	.493	.531	.561	.658	.738	.764	.770	.767
$\bar{g}/H_o$	2.78	2.81	2.80	2.77	2.73	2.70	2.55	2.34	2.20	2.10	2.03
$\bar{h}/H_o$	.781	.834	.862	.872	.876	.878	.873	.841	.811	.786	.767
Φ/Φ_o	33.2	22.0	14.8	11.9	10.2	9.19	6.71	5.03	4.28	3.85	3.57
$\kappa\Phi/\Phi_o$	.332	.439	.590	.711	.820	.919	1.34	2.01	2.57	3.08	3.57

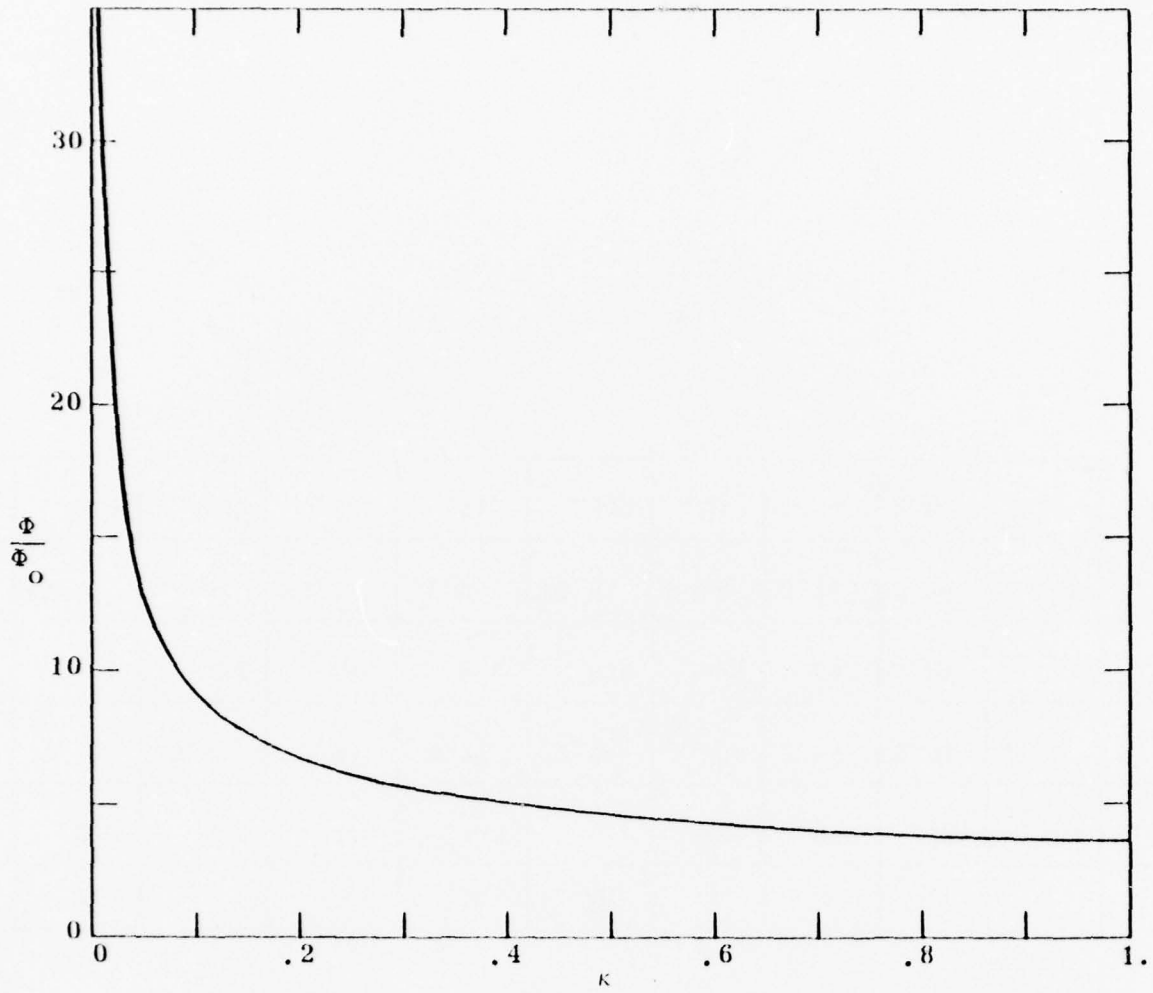

Figure 2. Flux Enbancement Factor Φ/Φ_o versus $\kappa = c/a$ for $a = b$ and $\mu = \infty$

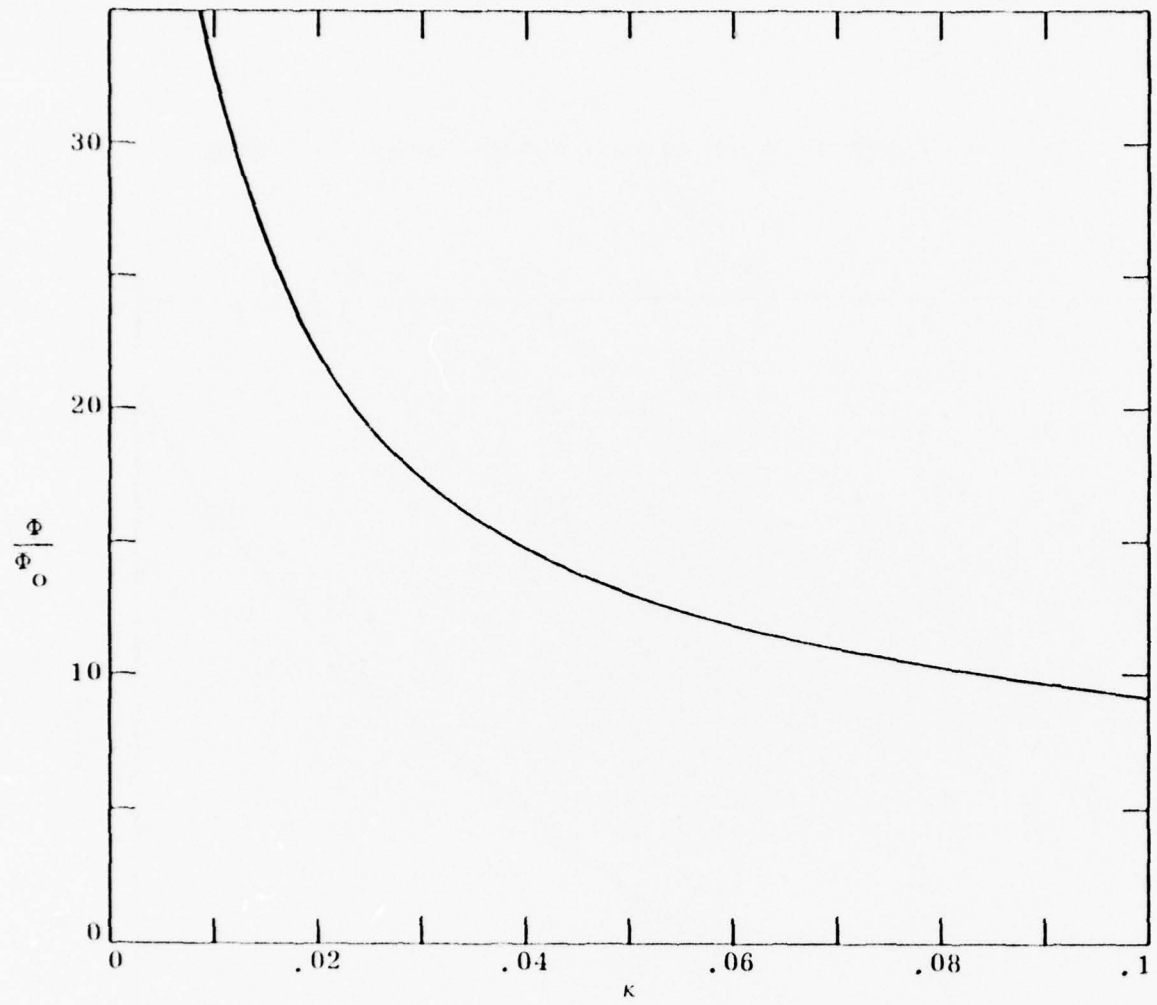

Figure 3. Flux Enhancement Factor Φ/Φ_o versus $\kappa = c/a$ for $a = b$ and $\mu = \infty$

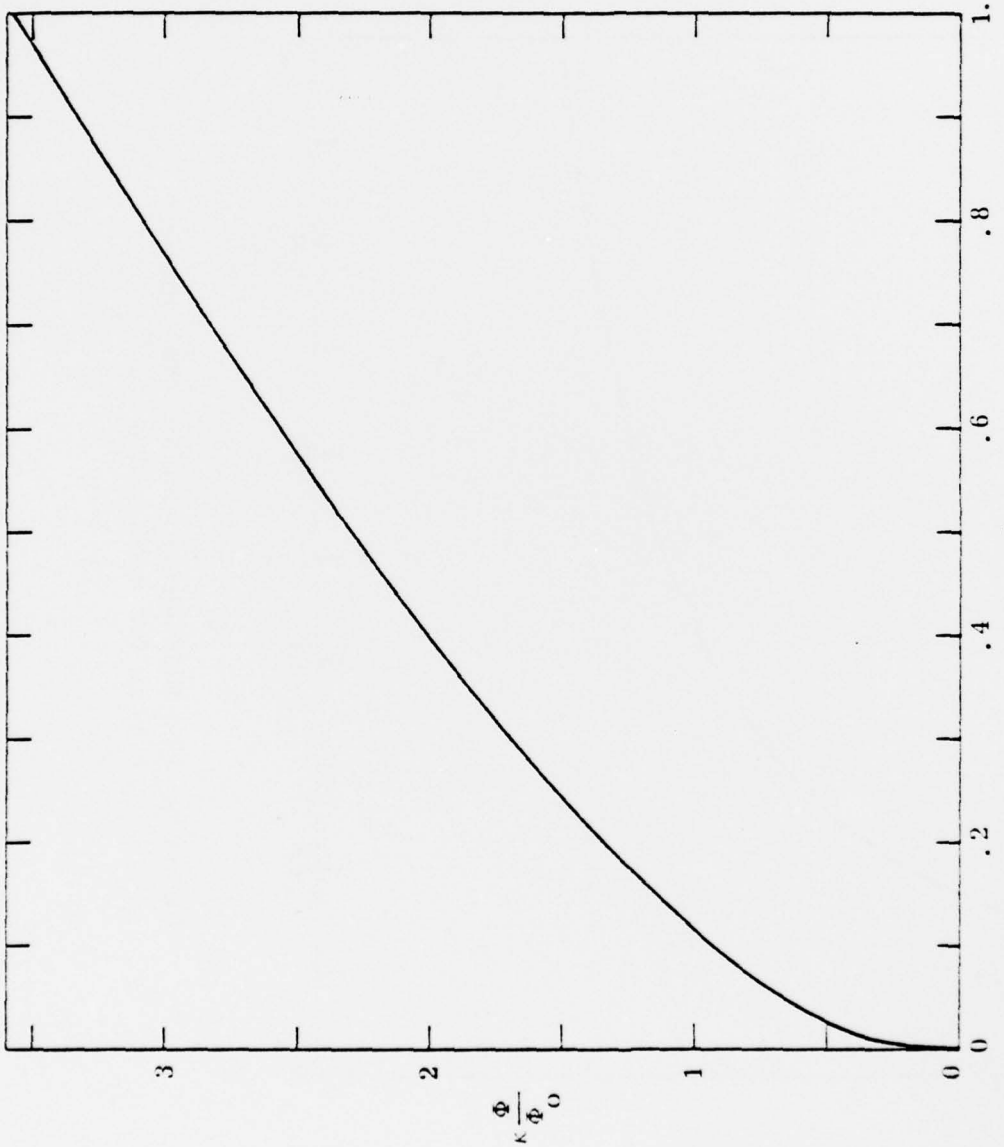

Figure 4. $\kappa\Phi/\Phi_o$ versus $\kappa = c/a$ for $a = b$ and $\mu = \infty$

SECTION VI

RECTANGULAR SOLID IN THE FIELD OF A RECTANGULAR CURRENT LOOP

Consider a thin-wire current loop wound tightly around the midsection of the rectangular infinitely-permeable solid. In Fig. 1 it is to be represented by the perimeter of the shaded area. We want to calculate the self-inductance of such a current loop. As is well known, our task amounts to calculating the total magnetic flux passing through the loop at unit current.

For a rectangular loop in free space lying in the y-z plane, defined by $y = \pm b'$ and $z = \pm c'$, and carrying a current I, the vector potential is easily found to be

$$\underline{A} = A_y \underline{e}_y + A_z \underline{e}_z \tag{28}$$

with

$$A_y(x, y, z) = \frac{\mu_o I}{4\pi} \ln \left(\frac{\left[x^2 + (y + b')^2 + (z + c')^2\right]^{1/2} + y + b'}{\left[x^2 + (y + b')^2 + (z - c')^2\right]^{1/2} + y + b'} \times \frac{\left[x^2 + (y - b')^2 + (z - c')^2\right]^{1/2} + y - b'}{\left[x^2 + (y - b')^2 + (z + c')^2\right]^{1/2} + y - b'} \right)$$

$$A_z(x, y, z) = \frac{\mu_o I}{4\pi} \ln \left(\frac{\left[x^2 + (y - b')^2 + (z + c')^2\right]^{1/2} + z + c'}{\left[x^2 + (y + b')^2 + (z + c')^2\right]^{1/2} + z + c'} \times \frac{\left[x^2 + (y + b')^2 + (z - c')^2\right]^{1/2} + z - c'}{\left[x^2 + (y - b')^2 + (z - c')^2\right]^{1/2} + z - c'} \right) \tag{29}$$

It is clear that for an infinitely thin wire, $\underline{A}$ diverges logarithmically at the wire. In order for (29) to represent the vector potential of a loop of small but finite wire radius R and wound tightly around a rectangular solid of cross-section b by c, we set

$$R = b' - b = c' - c \tag{30}$$

The magnetic field due to such a loop in free space is the incident field in the present problem, and is given by

$$\underline{H}^{inc}(\underline{r}) = \frac{1}{\mu_o} \nabla \times \underline{A}(\underline{r}) \tag{31}$$

It is clear that this problem possesses the same type of symmetry as the case of a uniform incident field treated in Section III, namely, the induced magnetic charge density on the solid's surface is again odd in x and even in y and z. The only difference is in the value of the incident field. Therefore in calculating the first iterated solution by the method of averaging functional corrections, we again arrive at (21) but with $\overline{F}_o$ given by

$$\overline{F}_o = \begin{pmatrix} 2\overline{H}_z^{inc} \\ 2\overline{H}_x^{inc} \\ 2\overline{H}_y^{inc} \end{pmatrix} \tag{32}$$

The averages are over the faces of the solid:

$$\overline{H}_z^{inc} = \frac{1}{2ab} \int_0^a dx \int_{-b}^b dy \, H_z^{inc}(z = c)$$

$$\overline{H}_x^{inc} = \frac{1}{4bc} \int_{-b}^b dy \int_{-c}^c dz \, H_x^{inc}(x = a)$$

$$\overline{H}_y^{inc} = \frac{1}{2ca} \int_{-c}^c dz \int_0^a dx \, H_y^{inc}(y = b) \tag{33}$$

Using (31) and Stokes' theorem, we obtain

$$\overline{H}_z^{inc} = \frac{1}{2ab\mu_o} \int_{-b}^b dy \left[A_y(a, y, c) - A_y(0, y, c) \right]$$

$$\overline{H}_x^{inc} = \frac{1}{2bc\mu_o} \left(\int_{-c}^c dz \, A_z(a, b, z) - \int_{-b}^b dy \, A_y(a, y, c) \right)$$

$$\overline{H}_y^{inc} = \frac{1}{2ca\mu_o} \int_{-c}^c dz \left[A_z(0, b, z) - A_z(a, b, z) \right] \tag{34}$$

For A_y and A_z given by (29) and b' and c' by (30), the integrals can be worked out analytically. We have

$$\int_{-c}^c dz \, A_z(a, b, z) = \frac{\mu_o I}{4\pi} W(a, b, c, R)$$

$$\int_{-b}^b dy \, A_y(a, y, c) = -\frac{\mu_o I}{4\pi} W(a, c, b, R) \tag{35}$$

where

$$W(a, b, c, d) = d\,\ell n\left(\frac{\left[a^2 + (2b + d)^2 + d^2\right]^{1/2} + d}{\left[a^2 + (2b + d)^2 + d^2\right]^{1/2} - d} \cdot \frac{\left[a^2 + 2d^2\right]^{1/2} - d}{\left[a^2 + 2d^2\right]^{1/2} + d}\right)$$

$$+ (2c + d)\,\ell n\left(\frac{\left[a^2 + (2c + d)^2 + d^2\right]^{1/2} + 2c + d}{\left[a^2 + (2c + d)^2 + d^2\right]^{1/2} - 2c - d} \cdot \frac{\left[a^2 + (2b + d)^2 + (2c + d)^2\right]^{1/2} - 2c - d}{\left[a^2 + (2b + d)^2 + (2c + d)^2\right]^{1/2} + 2c + d}\right)$$

$$- 2\left(\left[a^2 + (2b + d)^2 + d^2\right]^{1/2} - \left[a^2 + 2d^2\right]^{1/2} + \left[a^2 + (2c + d)^2 + d^2\right]^{1/2}\right.$$

$$\left. - \left[a^2 + (2b + d)^2 + (2c + d)^2\right]^{1/2}\right) \tag{36}$$

The *self-inductance in free space* L_o is the total flux through the loop at unit current and in the absence of the rectangular solid. We obtain

$$L_o = \frac{\mu_o}{I} \int_{-b}^{b} dy \int_{-c}^{c} dz\, H_x^{inc}(x = 0)$$

$$= \frac{2}{I}\left(\int_{-c}^{c} dz\, A_z(0, b, z) - \int_{-b}^{b} dy\, A_y(0, y, c)\right) \tag{37}$$

or, by (35),

$$L_o = \frac{\mu_o}{2\pi}[W(0, b, c, R) + W(0, c, b, R)] \tag{38}$$

On the other hand, by (16), the self-inductance L with the permeable core is

$$L = \frac{4ab\mu_o}{I}\left(\overline{f} + \frac{c}{a}\overline{g} + \frac{c}{b}\overline{h}\right) \tag{39}$$

SECTION VII

NUMERICAL RESULTS OF INDUCTANCE CALCULATIONS

For a case of immediate application we take a = b and R = a/900, and calculate the averaged vector $\overline{F}_o$ in (32) and L_o in (38) numerically as a function of the thickness-to-length ratio $\kappa = c/a$. The results are shown in Table 3. We then solve for $\overline{f}$, $\overline{g}$ and $\overline{h}$ from (21) and (32). The matrix $\overline{K}$ is as given in Table 1. The self-inductance L in (39) becomes in the present case

$$L = \frac{4a^2\mu_o}{I}[\overline{f} + \kappa(\overline{g} + \overline{h})] \qquad a = b \tag{40}$$

The numerical results are shown in Table 3. We also plot L_o in Fig. 5 and L in Figs. 6 and 7.

The curve for L exhibits a broad minimum at $\kappa \simeq 0.3$ and a sharp rise as $\kappa \to 0$. This behavior is at first puzzling since we more or less expect on intuitive grounds a monotonic dependence on κ. However, it is important to realize that the effect of κ on L arises from two sources: one directly from the geometry of the rectangular solid, and another indirectly from the incident field which varies with the loop geometry. To study the effect due purely to the solid, we must factor out that portion due to the incident field. Accordingly we calculate and plot the inductance enhancement factor L/L_o in Table 3 and Fig. 8. We see that this factor, purged of the κ-dependence from the incident field, is indeed a monotonic function of κ. It in fact closely resembles the flux enhancement factor Φ/Φ_o in Fig. 2. This result is remarkable since for Φ/Φ_o the incident

Table 3. Self-inductance enhancement factor L/L_o for a rectangular loop of wire radius R as a function of $\kappa = c/a$ for $a = b$, $R = a/900$ and $\mu = \infty$ ($\bar{f}$, $\bar{g}$, $\bar{h}$ and $\underline{\bar{\Pi}}^{inc}$ are in units of $I/4\pi a$, L and L_o in units of $\mu_o a/4\pi$).

κ	.01	.02	.04	.06	.08	.1	.2	.4	.6	.8	1.
$2\bar{\Pi}^{inc}_z$	11.74	14.37	17.00	18.52	19.57	20.37	22.63	24.32	24.91	25.17	25.29
$2\bar{\Pi}^{inc}_x$	.0795	.1510	.2935	.4346	.5739	.7107	1.343	2.268	2.793	3.075	3.227
$2\bar{\Pi}^{inc}_y$	11.21	13.55	16.01	17.46	18.48	19.26	21.56	23.52	24.43	24.95	25.29
L_o	23.71	29.29	35.31	39.19	42.19	44.73	54.41	69.26	82.49	95.18	107.6
$\bar{f}$	191	142	103	85.9	75.6	68.8	52.9	43.5	40.2	38.6	37.6
$\bar{g}$	508	317	188	136	108	89.5	49.8	27.9	20.4	16.6	14.4
$\bar{h}$	495	314	194	146	120	104	68.6	49.6	43.0	39.6	37.6
L	805	618	474	411	376	353	307	298	313	334	359
L/L_o	34.0	21.1	13.4	10.5	8.90	7.88	5.63	4.30	3.79	3.51	3.33

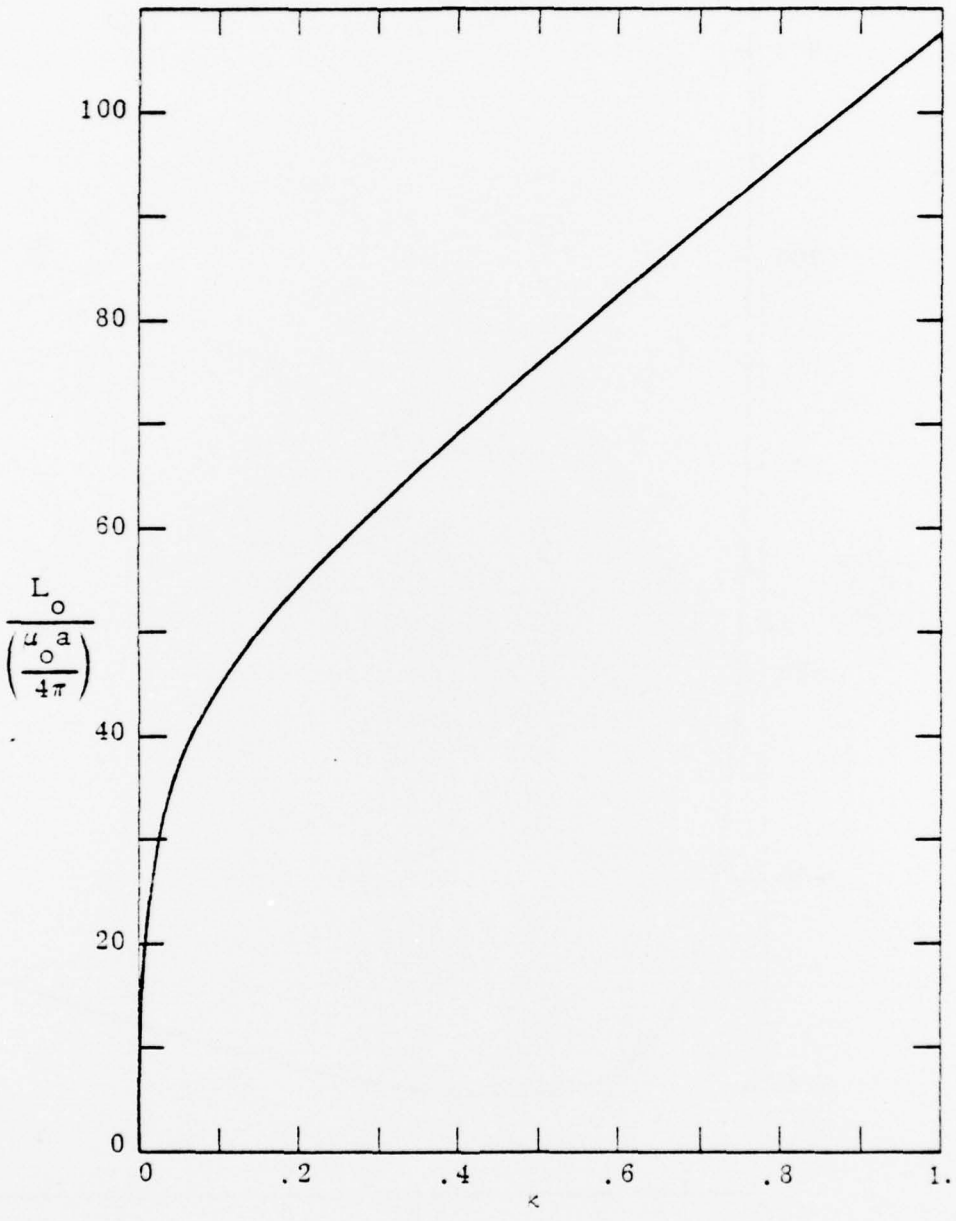

Figure 5. Self-Inductance in Free Space L_o versus $\kappa = c/a$ for $a = b$, $R = a/900$ and $\mu = \infty$

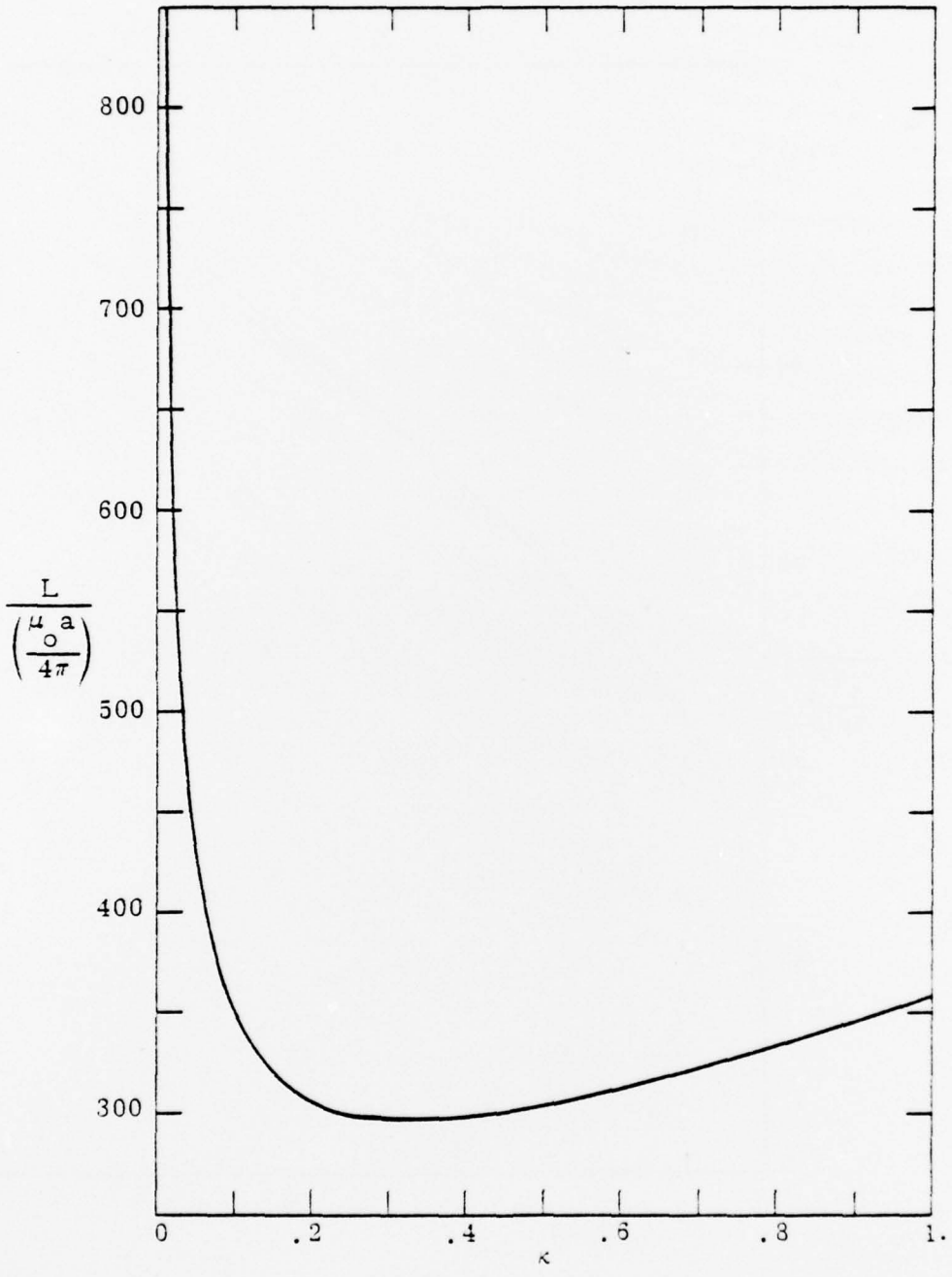

Figure 6. Self-Inductance with Rectangular Core L versus $\kappa = c/a$ for a = b, R = a/900 and $\mu = \infty$

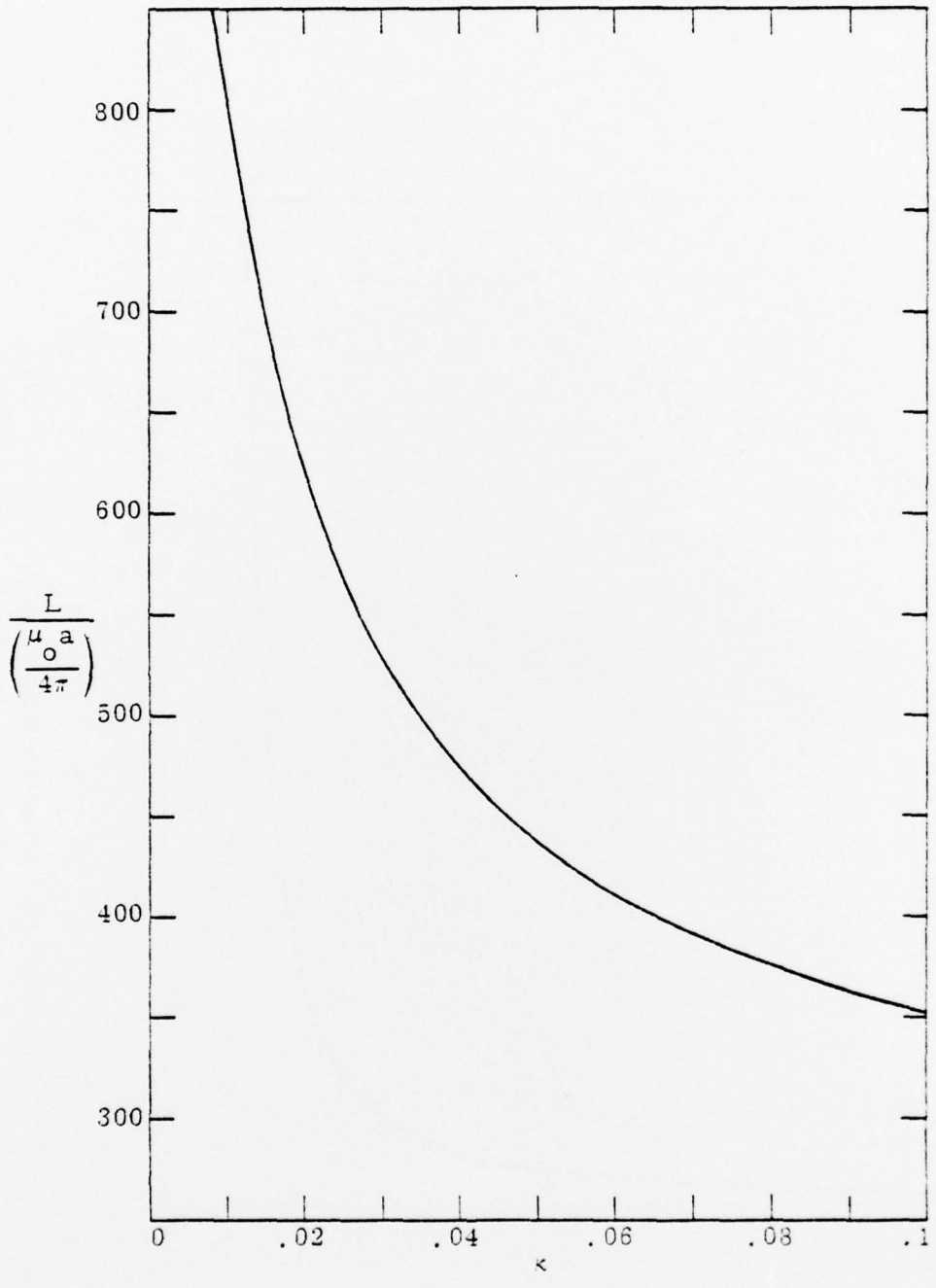

Figure 7. Self-Inductance with Rectangular Core L versus $\kappa = c/a$ for $a = b$, $R = a/900$ and $\mu = \infty$

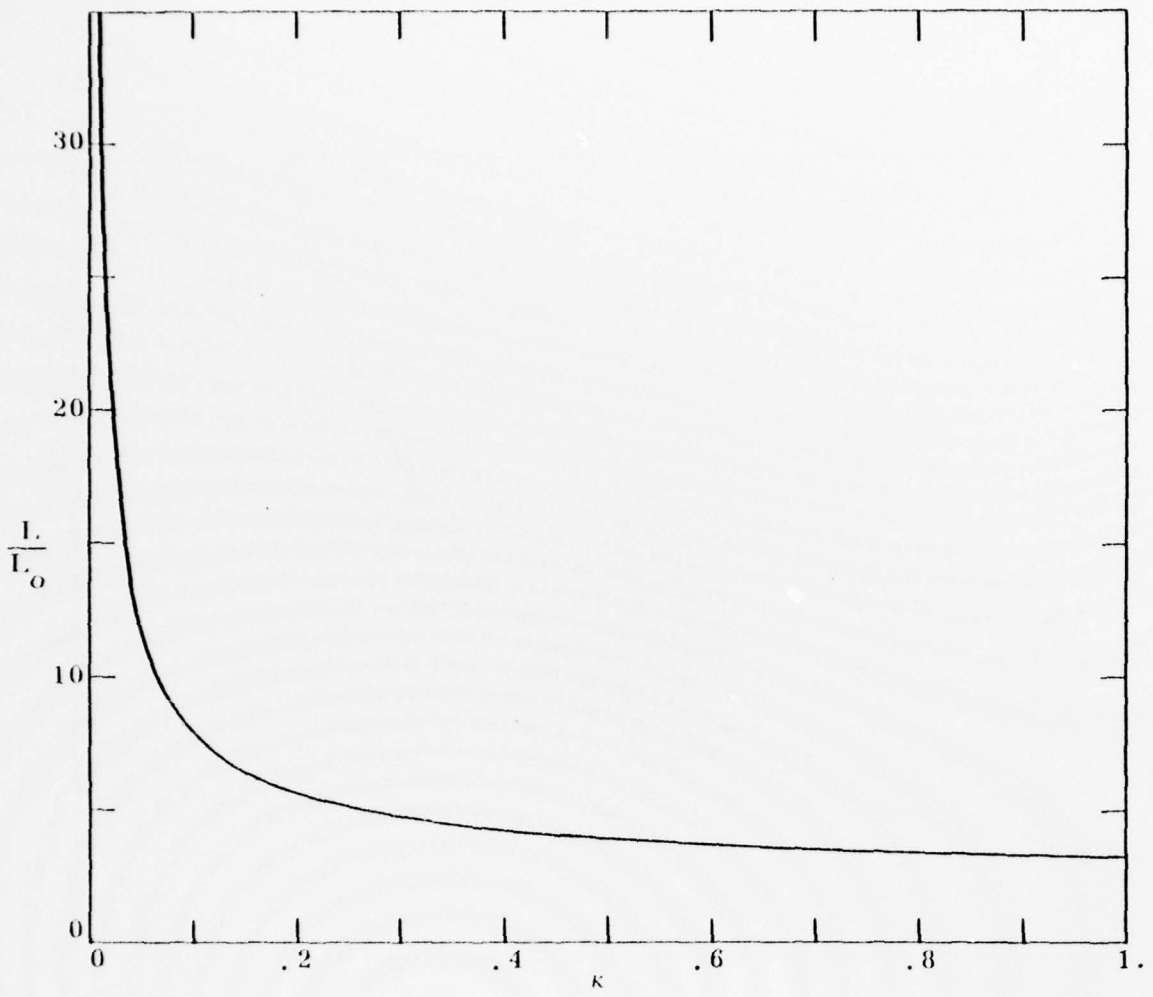

Figure 8. Self-Inductance Enhancement Factor L/L_o versus $\kappa = c/a$ for $a = b$, $R = a/900$ and $\mu = \infty$

field is purely in the x direction, whereas for L/L_o it is, by Table 3, predominantly in the y and z directions. It means that the flux amplification property of the rectangular permeable solid depends mainly on the total incident flux and not so much on the detailed configuration of the incident field.

From Fig. 5 we see that L_o is a monotonically increasing function of κ. If we write

$$L = \frac{L}{L_o} L_o \tag{41}$$

we can appreciate that L need not have any monotonic dependence on κ at all since it is the product of a monotonically decreasing and a monotonically increasing function. The sharp rise of L as $\kappa \to 0$ is really due to a faster rate of increase of L/L_o than the rate of decrease of L_o. We must also point out that for κ very close to 0, L must eventually come down to 0. This is because in this region L_o drops sharply to 0. In fact we have $L_o \sim \kappa |\ell n\, \kappa|$ while $L/L_o \sim |\ell n\, \kappa|$ for $\kappa \simeq 0$. This result is physically sound since the self-inductance of a current loop of zero area must be 0. On the other hand it is meaningless to push the present calculations down to very small κ. Our treatment of the current loop is based on the thin-wire approximation; this breaks down for $R \sim c$, when the thin wire must be considered as a massive cylinder.

Finally, what we have calculated is actually the external self-inductance. None of our results includes the internal self-inductance due

to magnetic flux in the interior of the thin wire. For a cylindrical thin wire of a non-magnetic conductor in free space, the internal self-inductance amounts to about $\mu_o/8\pi$ per unit wire length [5]. It is, however, negligible in our present problem.

SECTION VIII

CONCLUSIONS

The general problem of the interaction of a permeable solid with magnetic fields can be exactly formulated as a Fredholm integral equation of the second kind. While a number of numerical techniques are available for solving this type of integral equation, the method of averaging functional corrections is found to be particularly simple and powerful when it comes to evaluating the total magnetic flux passing through the solid. In this way, the total flux through a rectangular ferrite slab is calculated when the incident field is uniform and when it is generated by a rectangular current loop. It is found that a thin ferrite slab is a good flux concentrator.

REFERENCES

1. Luchka, A. Yu, The Method of Averaging Functional Corrections: Theory and Applications, Academic Press, New York, 1965.

2. Kellogg, O. D., Foundations of Potential Theory, Springer Verlag, Berlin, p. 164, 1929.

3. Noether, F., "Magnetostatik," In. P. Frank and R. von Mises, Die Differential-und Integralgleichungen der Mechanik und Physik, Band II, Friedr. Vieweg und Sohn, Braunschweig, p. 715, 1930.

4. Edwards, T. W., and J. van Bladel, "Electrostatic dipole moment of a dielectric cube," Appl. Sci. Res., 9B, pp. 151-155, 1962.

5. Smythe, W. R., Static and Dynamic Electricity, McGraw-Hill Book Co., Inc., New York, p. 317, 1950.